Presentation and interpretation of structural data from the Nagssugtoqidian orogen using a GIS platform: general trends and features

Jeroen A.M. van Gool and Sandra Piazolo

In this contribution we present data collected by more than 50 international geologists involved in geological mapping and research projects in the Nagssugtoqidian orogen of West Greenland, organised by the Geological Survey of Denmark and Greenland and the Danish Lithosphere Centre. Using a geographical information system (GIS) as a framework for visualisation and analysis of structural and lithological data, it is now possible to give a unique overview of thousands of data points, employed here within a study area of approximately 160 × 180 km in the central and northern Nagssugtoqidian orogen. The GIS methodology allows comparison, integration and analysis of datasets in terms of subject, space, and scale. This is extremely helpful in the recognition of geological patterns, such as terrain or domain boundaries and map-scale structures. Analysis of the available structural data shows clear differences in deformation patterns between the core and the northern segment of the Nagssugtoqidian orogen. One of the most prominent features is the ENE-striking Nordre Strømfjord shear zone, which transects the orogen from the coast to the Inland Ice. The data also clearly document a change from predominantly steeply dipping, ENE–WSW-trending fabrics and large, elongate structural domains in the core of the orogen, to large, open fold patterns and moderately to shallowly dipping fabrics in smaller structural domains in the north.

_____

J.A.M.v.G. & S.P., *Geological Survey of Denmark and Greenland, Øster Voldgade 10, DK-1350 Copenhagen K, Denmark.* E-mail: *jvg@geus.dk*
S.P., *Geological Survey of Denmark and Greenland, Øster Voldgade 10, DK-1350 Copenhagen K, Denmark.* Present address: *Department of Geology and Geochemistry, Stockholm University, 10691 Stockholm, Sweden.*

Over the past ten years the Nagssugtoqidian orogen in central West Greenland (Fig. 1) has been the subject of intense geological research, involving both bedrock mapping and research into the Palaeoproterozoic and Archaean tectonic evolution of the region. This has led to a major improvement in the understanding of the tectonic development of the Nagssugtoqidian orogen (Kalsbeek & Nutman 1996; Connelly *et al.* 2000; van Gool *et al.* 2002). The research was undertaken in two projects, organised by the Danish Lithosphere Centre (DLC) from 1994 to 1999 and the Geological Survey of Denmark and Greenland (GEUS) from 2000 to 2003, respectively. Approximately 35 international geologists from institutions on three continents participated in the field work of these projects, with changing teams from year to year. During these projects a very large amount of data was collected, including structural measurements, lithological observations, intrusive relationships, information about metamorphic mineral assemblages, etc. Other structural data were collected during previous work in part of the region in
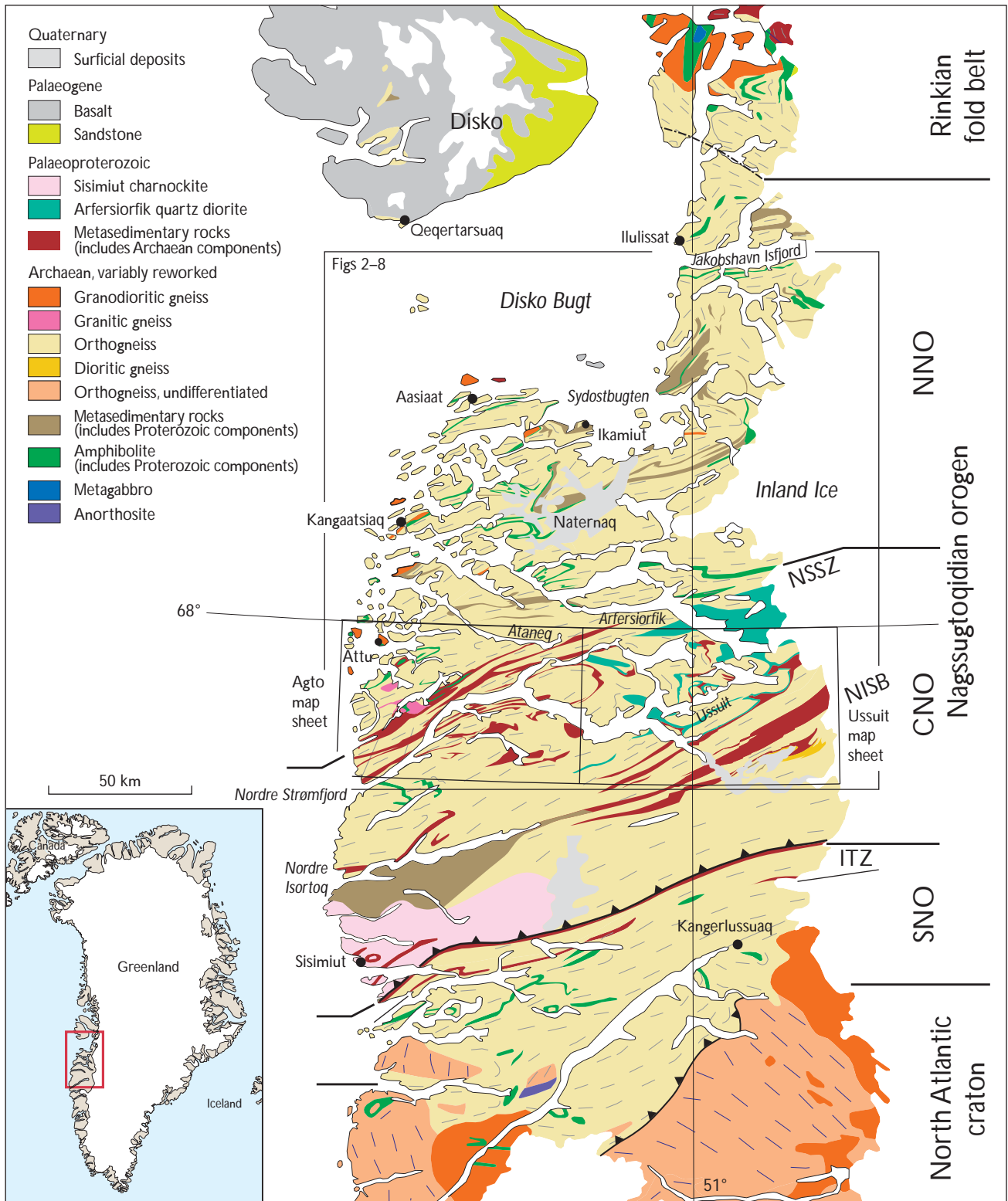
Fig. 1. Schematic geological map of central West Greenland (modified from van Gool *et al.* 2002), depicting the Nagssugtoqidian orogen. **ITZ**, Ikertôq thrust zone; **NISB**, Nordre Isortoq steep belt; **NSSZ**, Nordre Strømfjord shear zone; **SNO**, **CNO** and **NNO**, respectively, the southern, central and northern Nagssugtoqidian orogen. **Small boxes** outline the locations of the Agto and Ussuit map sheets; **Large box** indicates the location of Figs 2–8.

the 1960s and 1970s by the former Geological Survey of Greenland (GGU, now part of GEUS). Part of this was used by the collectors in their individual research or in small groups, and for the compilation of a published geological map, However, to date only a fraction of the total dataset has been made accessible in publications, and most of the original data collected prior to 2001 are only available for further analysis if extracted from the individual geologists' field diaries and field maps. With traditional methods it would be highly impractical and tedious to obtain an overview of all the structural data collected over time from the Nagssugtoqidian orogen in West Greenland, and a rigorous conventional analysis of the complete dataset would be close to impossible. Hence, alternative methods of data compilation and analysis were required.

Since 2001 GEUS' mapping projects have included systematic collection of structural data which are available digitally. The data from all participants are recorded in field diaries and on maps, stored electronically in spreadsheets, and subsequently entered in a geographical information system (GIS) for further presentation and analysis. In this way all data from an entire group of geologists can be accessed as a whole and used for map production and data analysis.

GIS methods has already proved useful in several disciplines including mineral exploration on local to global scales (e.g. Bonham-Carter *et al.* 1990; Goodwin *et al.* 1996; Knox-Robinson & Wyborn 1997; Harris *et al.* 2001), palaeontology (e.g. Carrasco & Barnosky 2000), and environmental assessment (e.g. True *et al.* 1999; Books 2000; Wilson *et al.* 2000).

In this paper we demonstrate the application of GIS data management, visualisation and methods of analysis in a large-scale and long-term international project, including data from two previous mapping projects in the region. We present for the first time in a digital format a set of more than 10 000 structural orientation measurements and observations collected by more than 50 geologists in the Nagssugtoqidian orogen over a period of 40 years. Such a presentation can (a) provide a very helpful overview of the data itself, (b) help to identify where future research efforts may be scientifically interesting, and (c) show how these together with geological and geophysical maps can define structural domains and illustrate the large-scale structural variations through an important part of the orogen.

The Nagssugtoqidian orogen

The Nagssugtoqidian orogen in West Greenland is a Palaeoproterozoic collisional belt, dominated by Archaean gneisses that were reworked at amphibolite and granulite facies during the Palaeoproterozoic orogeny (van Gool *et al.* 2002). It forms the northern boundary of the North Atlantic craton in southern Greenland, and is bound to the north by the contemporaneous Rinkian fold belt. It consists of three tectonic segments, referred to as the southern, central and northern Nagssugtoqidian orogen (SNO, CNO and NNO; Fig. 1), which respectively consist of a southern parautochthonous foreland, a high-grade core, and a transition zone to the Rinkian fold belt. Juvenile Palaeoproterozoic magmatic arc rocks and supracrustal sequences occur mainly in narrow belts within the CNO. The Nagssugtoqidian orogen is characterised by a dominant ENE–WSW structural trend, which culminates in a number of linear belts: the Ikertôq thrust zone, the Nordre Isortoq steep belt, and the Nordre Strømfjord shear zone. These are interpreted as crustal-scale structures and alternate with areas dominated by large fold structures. Detailed investigations in the core of the orogen have shown that during the Nagssugtoqidian orogeny this region originally underwent a phase of NW-vergent thrusting, followed by folding now recognised predominantly as isoclinal folds (van Gool *et al.* 2002). A second fold phase resulted in upright, ENE-trending folds on a scale of tens of kilometres, with associated development of extension lineations plunging shallowly ENE. Finally, a phase of sinistral strike-slip shearing on the steep flanks of the large fold structures resulted in the above mentioned prominent linear belts. It is therefore only the latest deformation phases that generated the main ENE–WSW-trending tectonic fabric of the orogen (van Gool *et al.* 2002).

The area discussed in this study extends from 67°N in the Nordre Strømfjord region to 69°10′N at Jakobshavn Isfjord and covers the northern part of the CNO and most of the NNO (Fig. 1).

Structural data

Origin of the data

The structural data have been derived from two different sources. The data north of 68°N were collected during recent GEUS mapping projects (2001–2003), while the data from south of 68°N have been extracted from published GGU and GEUS maps, collected during previous GGU, DLC and GEUS projects. During the recent GEUS

mapping projects, data were collected in the northern Nagssugtoqidian orogen. Structural measurements and other geological data were noted in field diaries together with their geographical coordinates using global positioning system (GPS) receivers. These data were subsequently entered in spreadsheets and imported into ArcView®. The geographical distribution of the structural data reflects the way they were collected along shorelines and on inland traverses. There may be several measurements at any one location, whereas no data were obtained in areas between traverses (which were often located many kilometres apart). In this study, we have restricted our analysis to the structural measurements. However, a combination of these data with other information, e.g. lithological and geophysical data, would make this GIS-based analysis tool even more powerful.

The southern part of the study area, south of 68°, is covered by two 1:100 000 scale maps, which were compiled prior to the digital storage of field data. The Agto map sheet in the west (Olesen 1984) consists of analogue data (but was recently digitised), whereas the Ussuit map sheet in the east was produced in digital format (Fig. 1; van Gool & Marker 2004). The structural data from the Agto and Ussuit map sheets are stored in GEUS' Geogreen map database and were extracted from this for the present study. However, these structural data only represent a fraction of the original data collected in the field. During the map compilations, the original structural data recorded on field maps or noted field diaries were filtered such that only representative measurements were shown on the final map; each measurement typically covers an area of a few square kilometres. Thus, the southern part of the data compilation map in this paper shows an even distribution of data, and a much lower data density, compared to the more recently compiled areas in the north. The fact that the Agto map sheet only contains very few lineation measurements compared to the surrounding regions also reflects a change in focus since the 1960s and 1970s, when measurement of lineations was not considered a high priority. A large gap in the data coverage occurs in the east, from Arfersiorfik fjord to the north almost up to Sydostbugten (Fig. 1); this area was not covered by the mapping programmes by GGU and GEUS.

Definition of terms

In the descriptions below the general *orientation* of a structural element is its three-dimensional orientation with respect to true north and horizontal, as defined by the combination of strike, dip direction and dip for planar
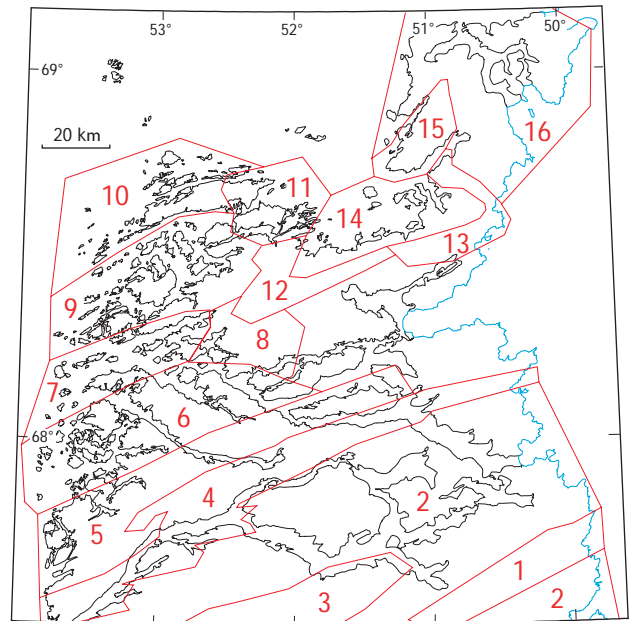

Fig. 2. Structural domains in the central and northern Nagssugtoqidian orogen, based on structural orientation data. Domain numbers refer to those used in Table 1, Fig. 8, and the main text.

structures, and plunge direction and plunge for linear structures. the term *trend* is used as the direction along the strike of a planar structure (without indication of dip direction), or the direction of plunge of a linear structure, without distinction between plunges up or down this direction. The trend is always expressed as two opposite directions (e.g. NE–SW).

Methods of data presentation

For map presentation of the data we have used ArcView® version 3.2. In addition, stereographic projections and statistical analysis for the determination of great circles and point maxima were prepared with StereoNett (J. Duyster, unpublished freeware). Once the structural dataset has been incorporated into the GIS database, the ArcView® Geoprocessing extension can be used to easily select subsets of data in areas with irregular shapes (Fig. 2), or alternatively functions like ArcView® Query Builder can be used to select data with certain characteristics.

The data were plotted on a topographic map using conventional structural symbols, whereas orientations and dip angles were colour-coded. For foliations and lineations, four maps with different colour codes were plotted (Figs 3–7). Having attempted several different ways of displaying variations of dip/plunge directions on maps, we found
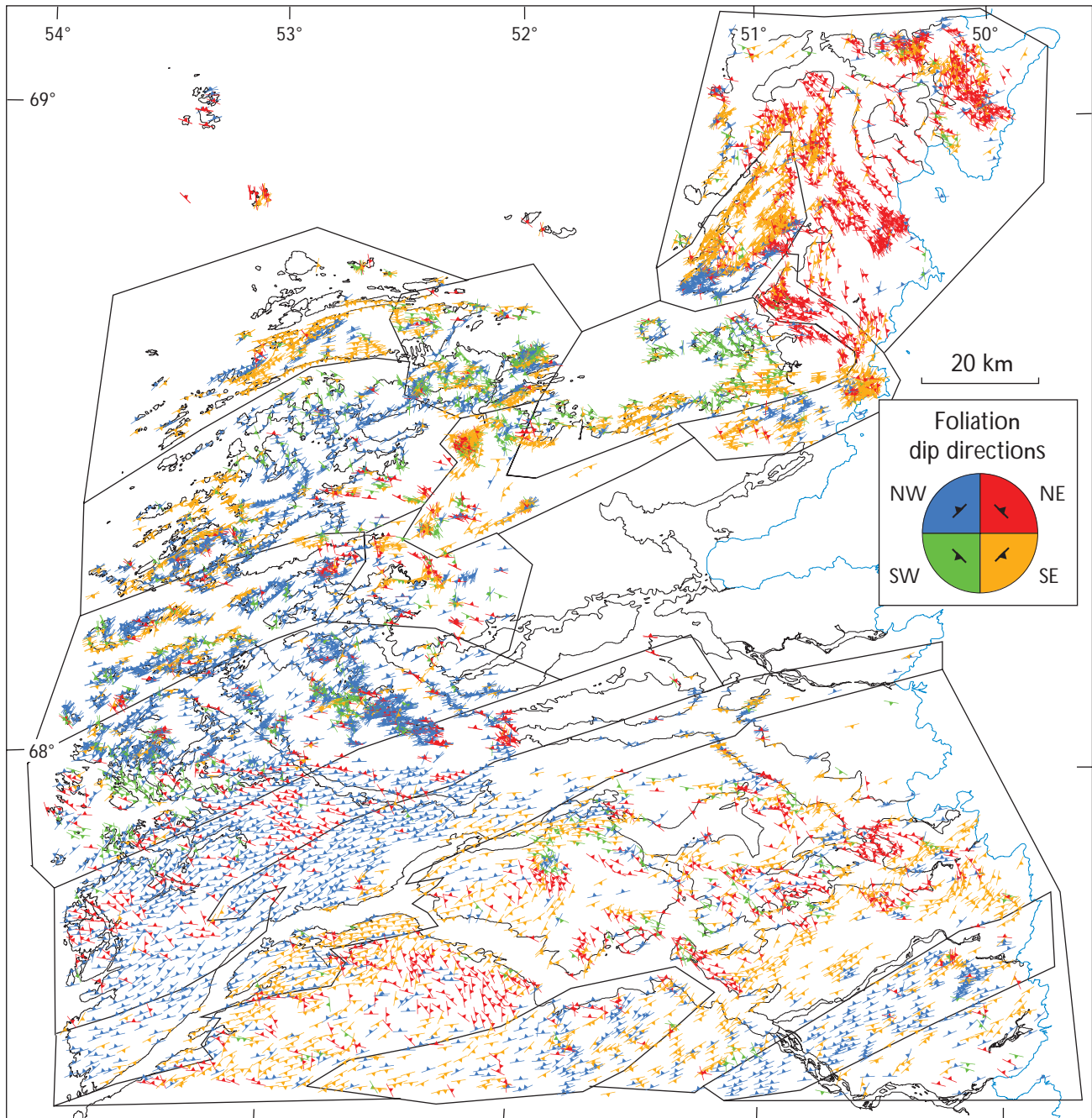
Fig. 3A. Foliation data, using four different colours to represent dip directions in the four quadrants of 0–90°, 90–180°, 180–270° and 270–360°.

that the regional trends were best shown using a subdivision into colour-coded quadrants. This gives a clear indication of variations on a regional scale and displays features that conventional plots of structural data would not have easily revealed. Other features of the data could be highlighted with other methods of coding, or by plotting them on a different scale. The GIS program allows the user to change the coding criteria and colours with a lim-

ited number of key strokes, and thus forms a powerful, user-friendly tool of analysis.

We plotted one map for each of the planar and linear datasets (Figs 3A, 5A), using differently coloured symbols for dip/plunge directions within each of four different quadrants: directions between 0–90° (NE quadrant) are shown in red, 90–180° (SE quadrant) in orange, 180–270° (SW quadrant) in green, and 270–360° (NW quad-
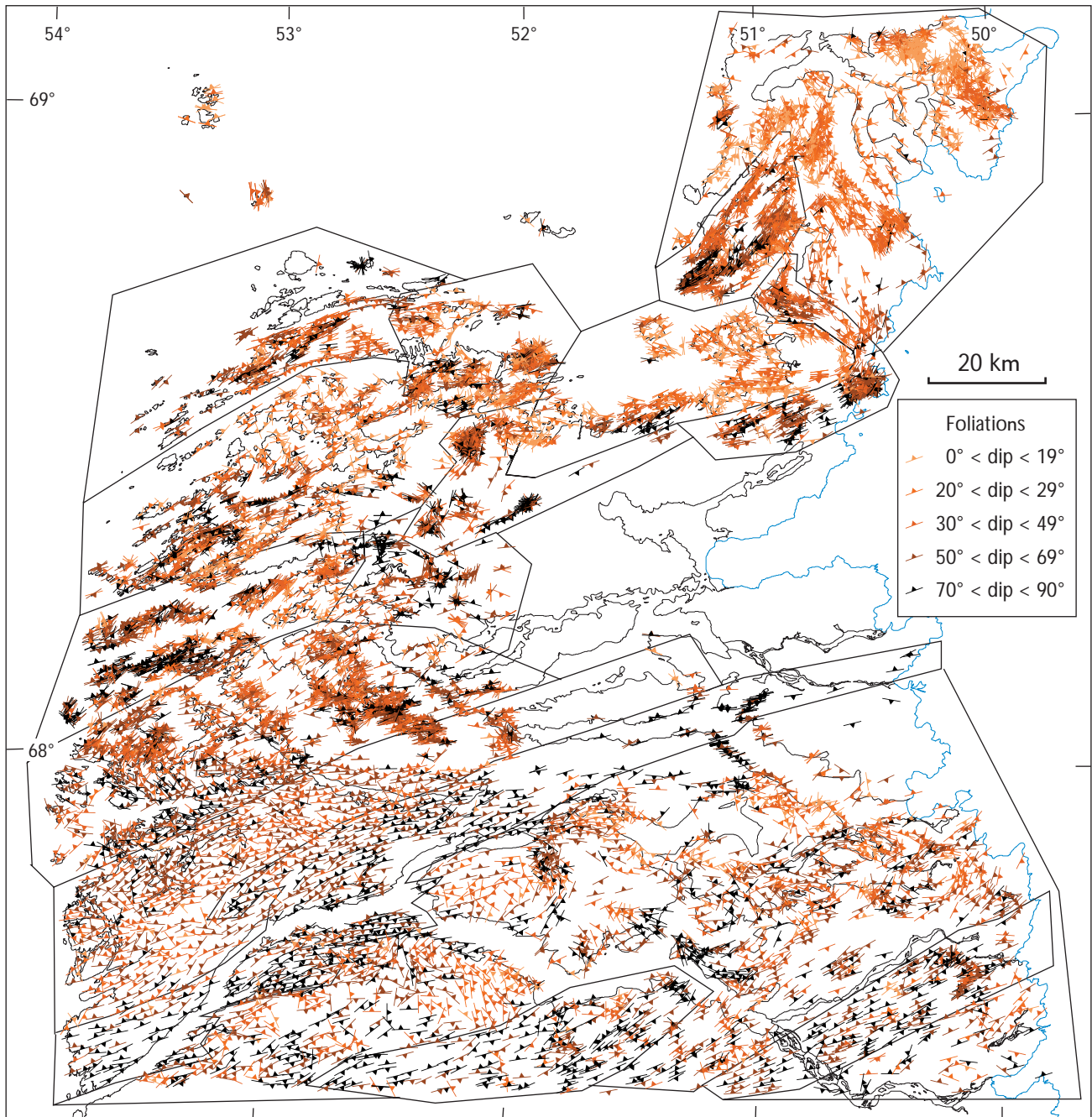
Fig. 3B. Foliation data, using colour intensity to reflect dip angle. Darker colours indicate steeper dip angles.

rant) in blue. We also plotted foliations, lineations and fold axes, respectively, in three maps where the colour intensity reflects the steepness of the dip/plunge (Figs 3B, 5B, 7). Here the light orange colour indicates shallow dips/plunges, and darker brown to black colours indicate progressively steeper dips/plunges.

The data were also plotted in a third way by combining the two just described methods. The different colours were maintained for the dip/plunge directions within each of the four quadrants, combined with colour intensity to display the variations in dip. The foliation data were split into two separate plots to show more detail and avoid clutter: Fig. 4A shows the overall ENE–WSW-trending structures (blue and orange), whereas Fig. 4B contains the overall ESE–WNW-trending structures (red and green). A similar method was used for the lineations, however, on
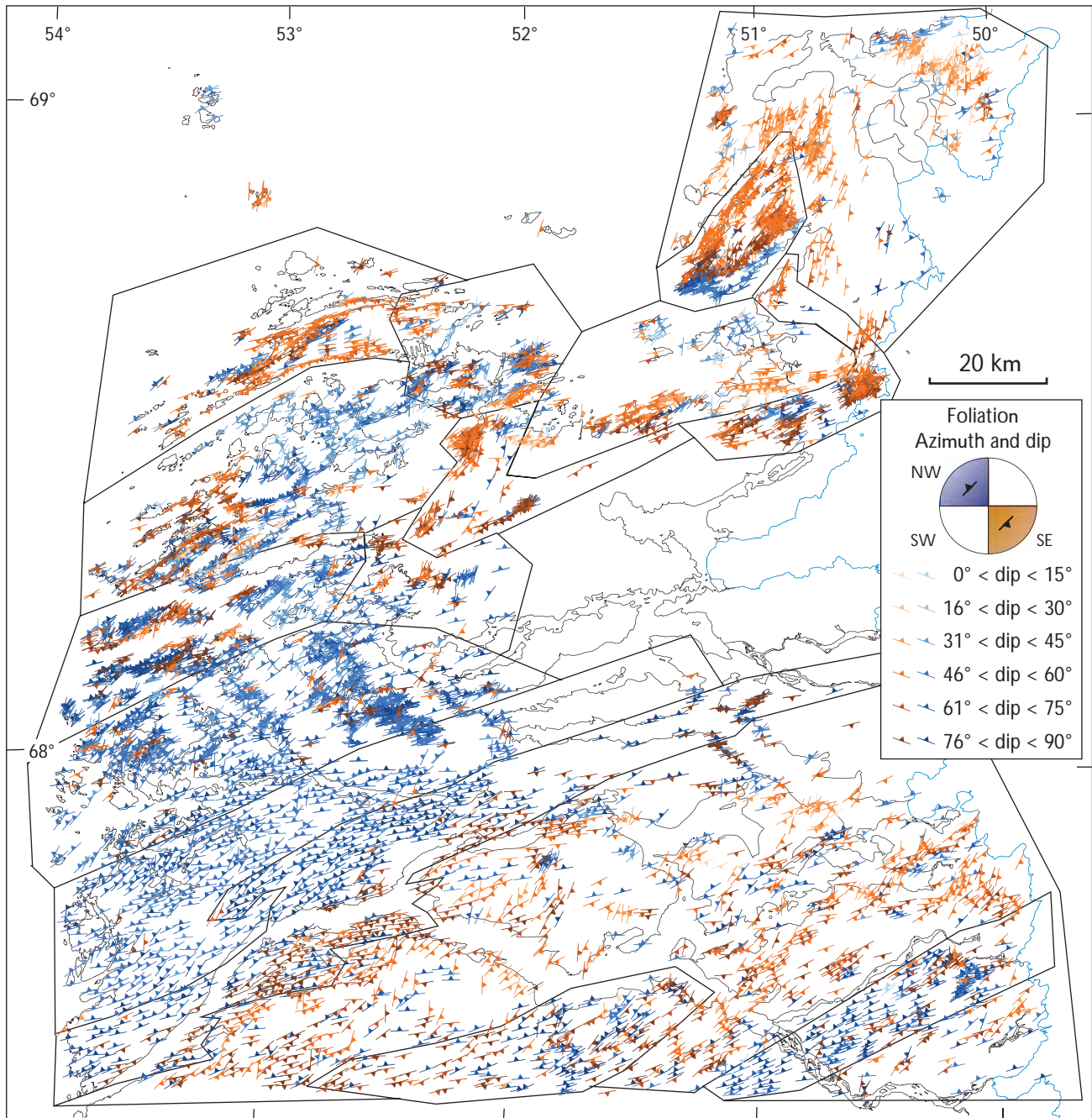
Fig. 4A. Foliation data, using blue and orange colours for NE–SW trends with NW and SE dips, respectively, combined with colour intensity to reflect dip angle. See Fig. 4B for NW–SE trends.

the scale of presentation many of the red and green lineations (ENE–WSW-trending) would overlap. Therefore, the green symbols were plotted separately (Fig. 6A), whereas the red symbols were included with the blue and orange ones (Fig. 6B); there are relatively few blue and orange symbols and therefore less cluttering.

There are significantly less measurements of fold axes than of other structural elements. Therefore we were not able to use their orientations for analysis of regional trends, and the fold axes are only colour coded for plunge angle (Fig. 7).

In some areas the very high data density causes a saturation with the colour of the main orientation on the scale of presentation. Although the main trends can still be seen, minor orientation components may be obscured. This problem can be overcome by zooming in on smaller areas
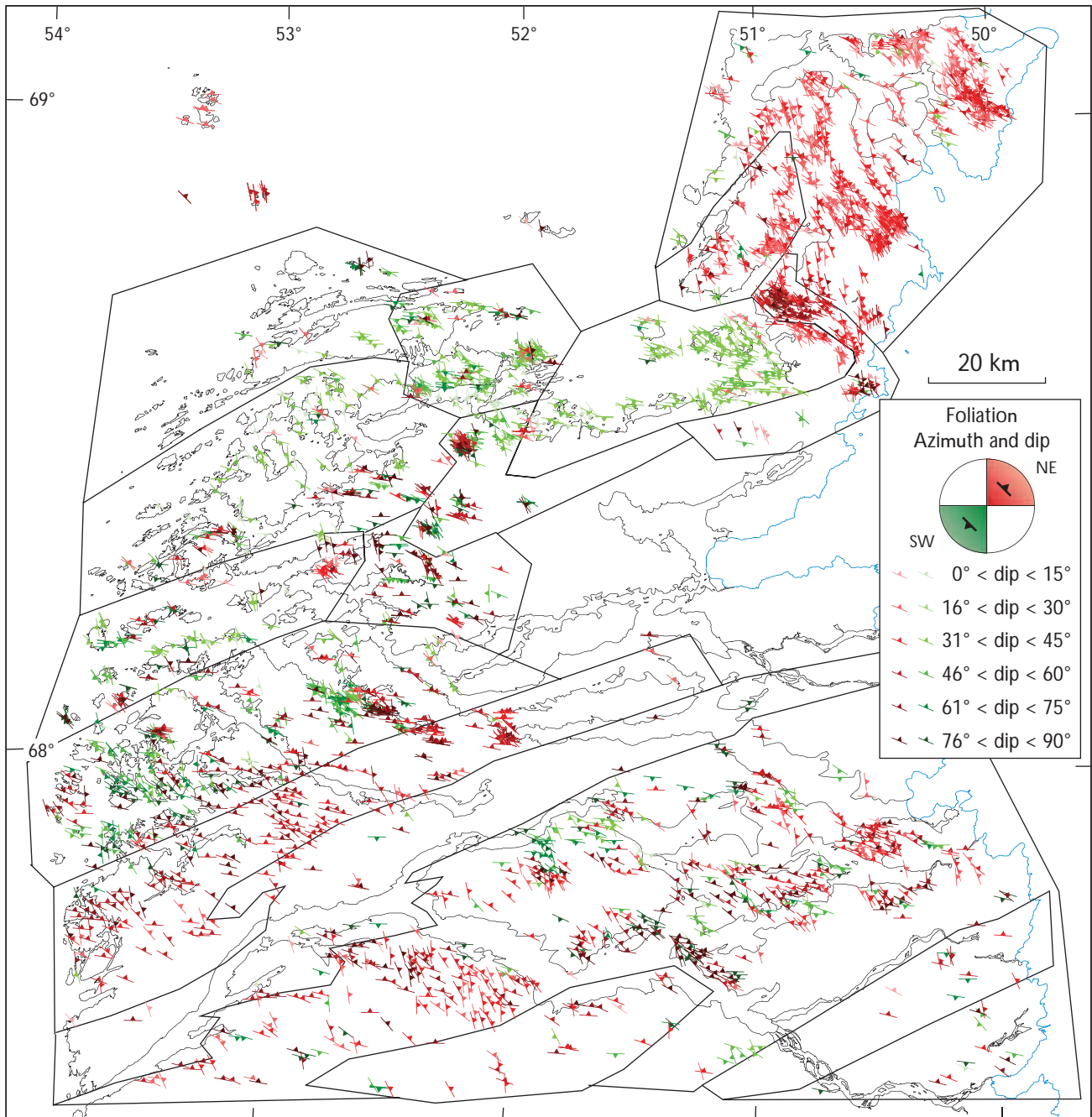
Fig. 4B. Foliation data, using red and green colours for NW–SE trends with NE and SW dips, respectively, combined with colour intensity to reflect dip angle. See Fig. 4A for NE–SW trends.

and printing on a different scale, revealing the full range of the data (e.g. Mazur *et al.* 2006, this volume).

Structural domains

Apart from the general variations in structural style, it is apparent that there are well defined areas with distinct structural patterns. We therefore divided the whole study area into 16 structural domains (Fig. 2), within each of which the structural characteristics are largely consistent and more or less distinct from those of adjacent domains. this subdivision is exclusively based on visual evaluation of the plotted data. A more rigorous approach for the definition of domains would have been possible, for example the method by Vollmer (1990) based on eigenvalue cal-
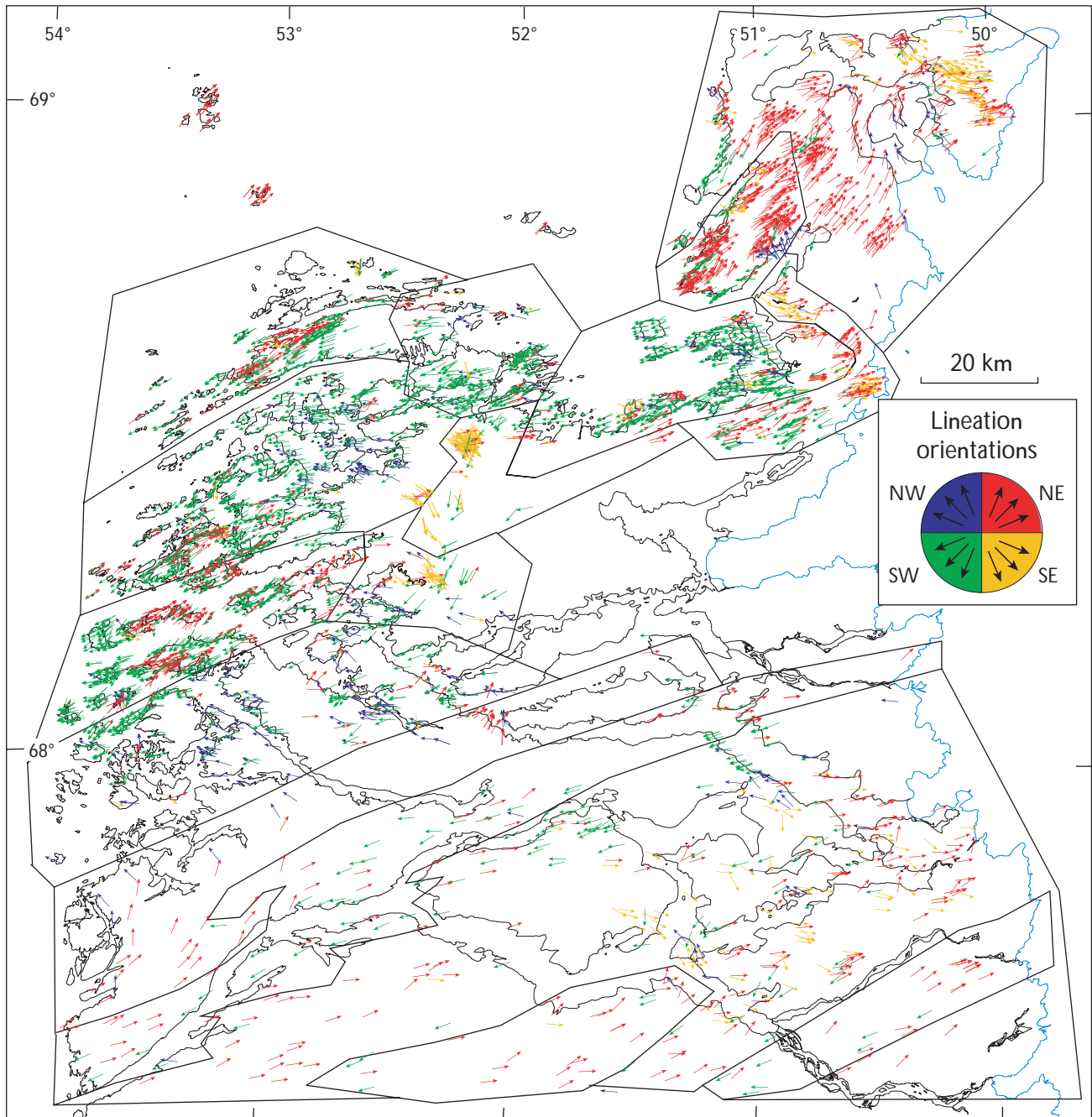
Fig. 5A. Lineation data, using four different colours to represent plunge directions in the four quadrants of 0–90°, 90–180°, 180–270° and 270–360°. See also Fig. 5B.

culations of data in small subsets, but is beyond the scope of the present study. The domains are presented schematically in Fig. 2, and their outlines are also shown in Figs 3–8. The structural data for each of the domains were extracted and plotted as equal area, lower hemisphere stereographic projections (Fig. 8). Foliations were plotted as poles to planes and contoured, and the orientation of the maximum density of data indicated in each plot. Great circles were calculated where visual inspection of the contoured data suggested that a great circle distribution exists. Calculations of great circle and fold axis orientations are based on the orientations of the three eigenvectors of the data. The large number of data in the contoured plots results in an accentuation of the high concentrations, while smaller populations that define separate structures are less visible. However, these are included in the calculations of
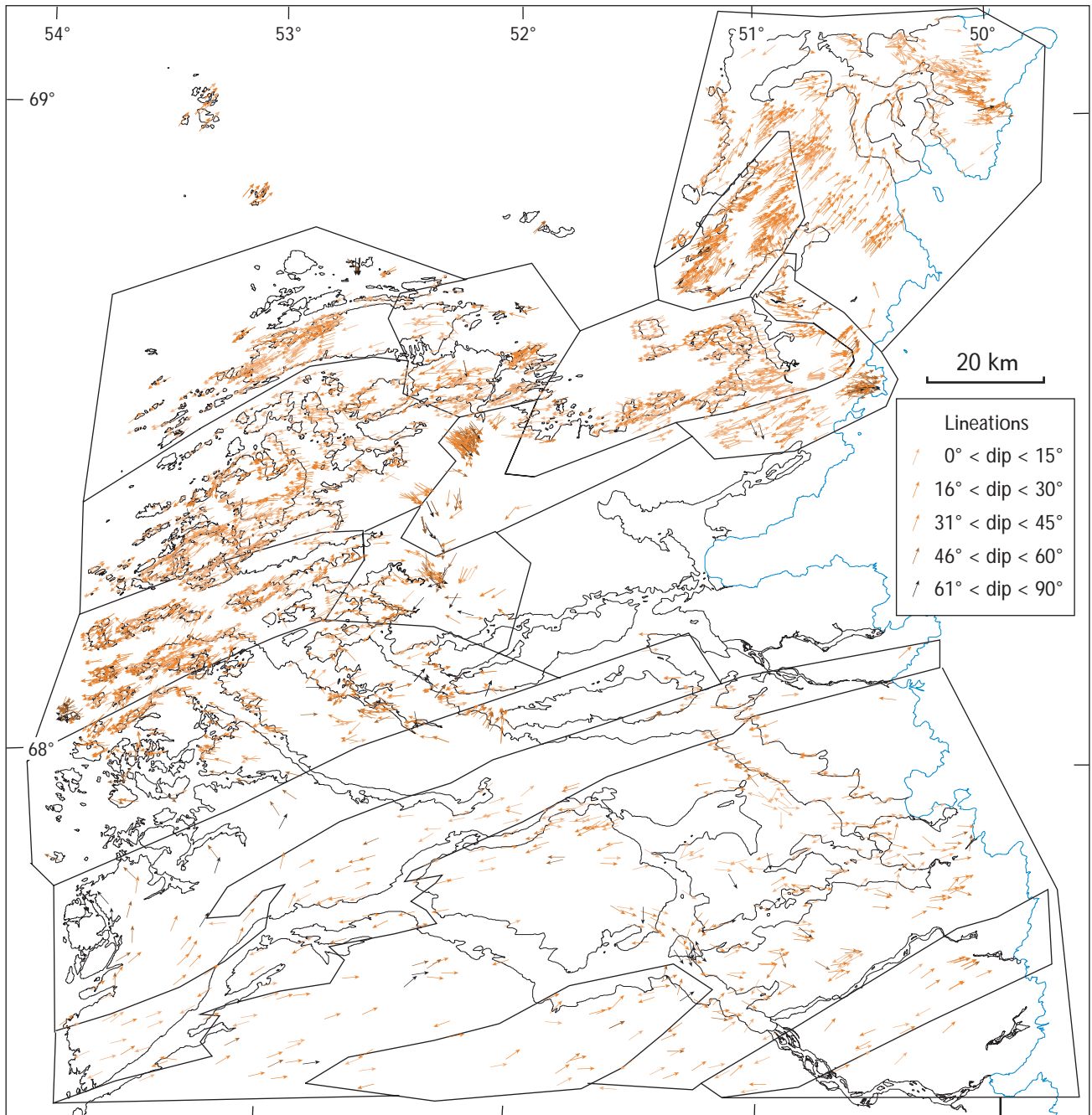
Fig. 5B. Lineation data, using colour intensity to reflect steepness of plunge. See also Fig. 5A.

the great circles and fold axes, and therefore the calcula-ted great circle may diverge from the one defined by the maximum orientations, as in domains 7, 9 and 14 (Fig. 8). Lineations were plotted and contoured, with indica-tion of the orientation of the maximum concentration of data (Fig. 8B). Table 1 contains short descriptions of the characteristics of each domain regarding foliation, linear data and general geology.

Results

The main variations in the structural patterns within the study area are described in the following sections, using structural maps and stereographic projections (Figs 3–8). The structural variations are apparent at a first glance as clustering of data and variations in colours; they reflect the nature of the large-scale tectonic evolution of the oro-gen, which is discussed in a final section.
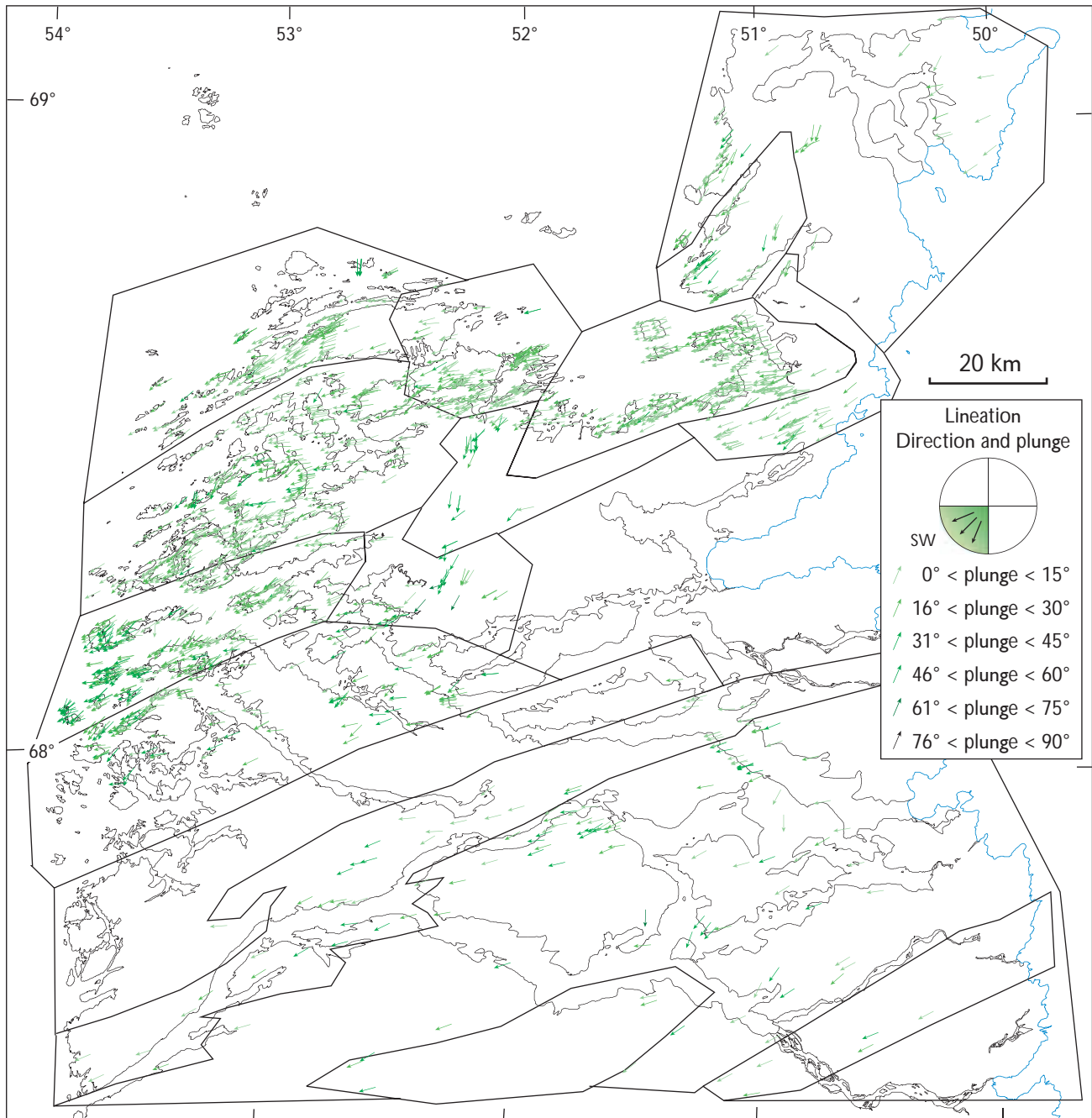
Fig. 6A. Lineation data, using green colour to represent SW directions and colour intensity to reflect steepness of plunge. See Fig. 6B for NW, NE and SE directions.

Foliations

Overviews of the orientations of the planar fabrics are shown in Figs 3, 4. The predominant foliation trend is ENE–WSW, shown in orange and blue colours. Linear belts in this direction, dominated by steeply dipping foliations, alternate with broader regions characterised by strongly variable orientations. These belts and regions with different structural characteristics have previously been referred to as steep belts and flat belts, respectively (Marker *et al.* 1995). The distinct alternation between such distinct linear belts and folded regions diminishes towards the north, and the predominant general ENE–WSW trend becomes progressively weaker, as reflected by the increase of red- and green-coloured symbols. This is apparent especially in the north-eastern corner of the study region, where the foliations are dominated by NE dip directions
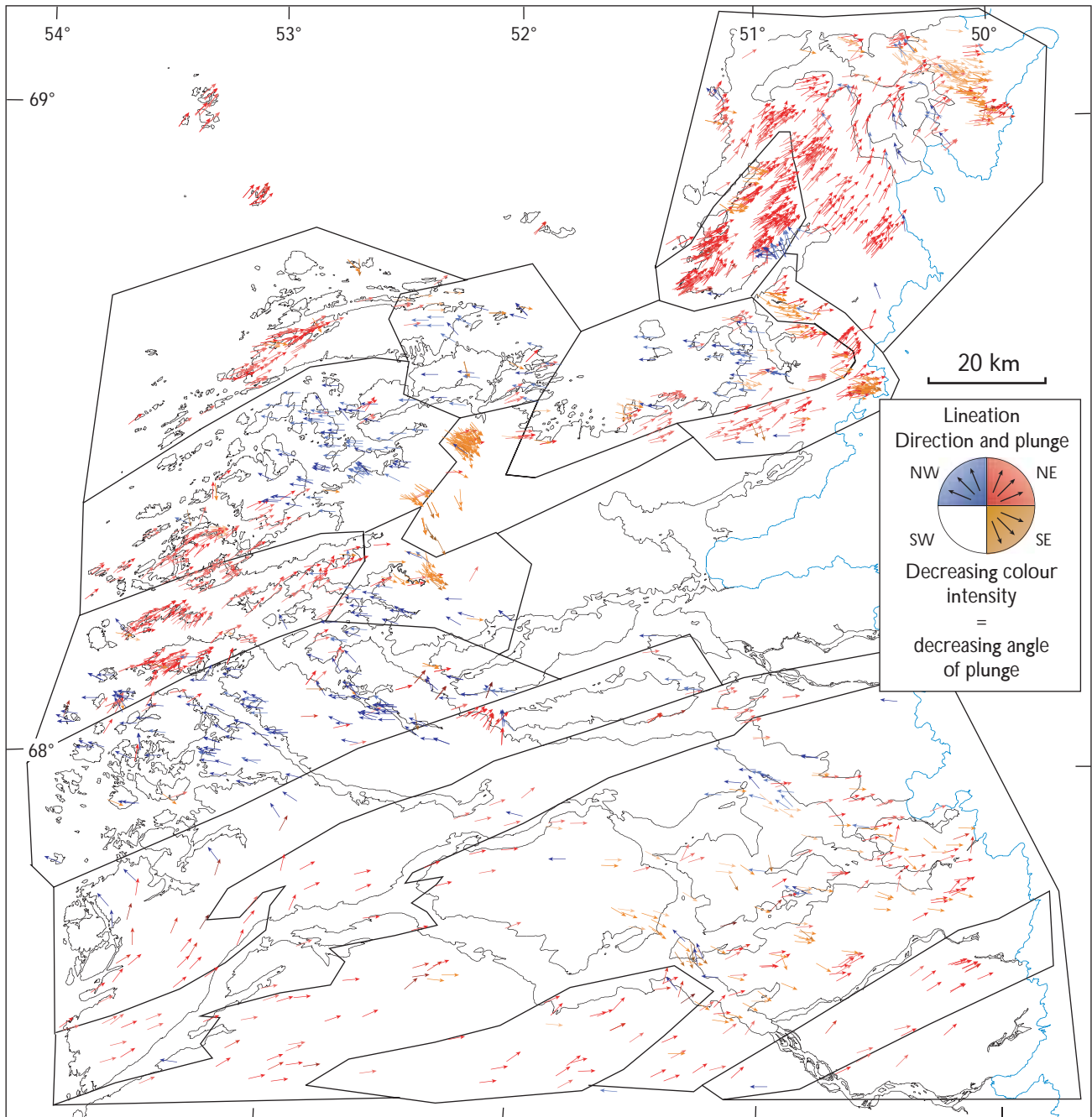
Fig. 6B. Lineation data, using blue, red and orange colours for NW, NE and SE orientations, respectively, combined with colour intensity to reflect steepness of plunge. See Fig. 6A for SW directions.

shown in red. Coupled with this progressive change towards the north there is an overall decrease in the dip angle, as expressed by an increasing amount of light orange-coloured symbols.

In the south, the two main linear belts, the Nordre Isortoq steep belt in domain 1 and the Nordre Strømfjord shear zone in domain 4, are characterised by a near-uniform ENE–WSW-trending foliation, a marked absence

of NW–SE-trending foliations, and steep dip angles. A third linear belt in the north, the Naternaq belt in domains 12 and 13 and the northern part of domain 7, is discontinuous and less well defined. Smaller, discontinuous shear zones also occur in the NNO e.g. in domains 10 and 15; these are indicated by strong clustering and alignment of symbols of the same colour, but not necessarily by steep dips. Dip directions of the overall ENE–WSW-trending
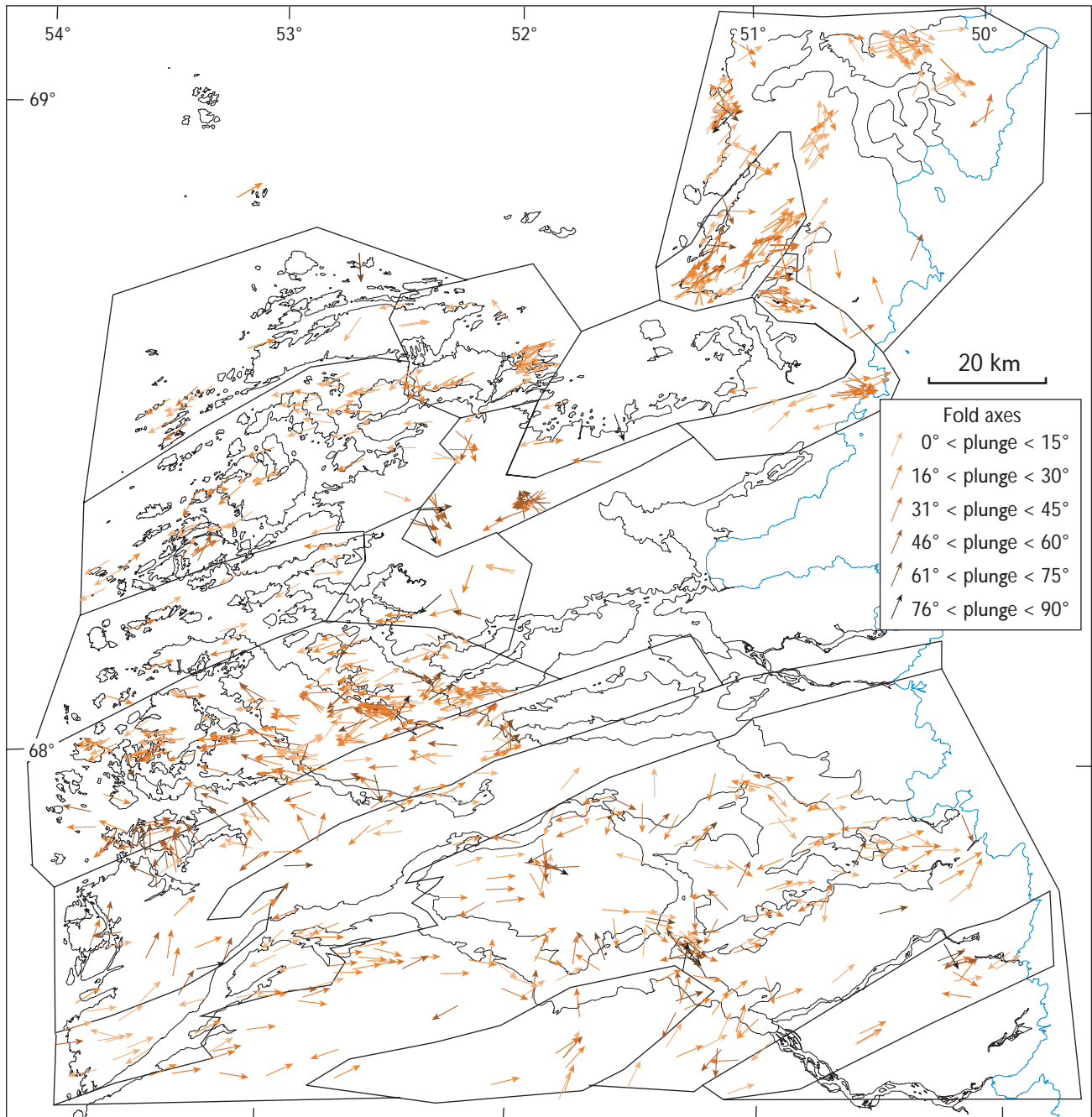
Fig. 7. Fold axis data, using colour intensity to reflect steepness of plunge.

structures (in blue and orange colours, Fig. 3A) show a clear regional pattern of alternating NW and SE dip directions. In the south, switches in dip directions are associated with the two main linear belts such that the intervening area, which forms a large anticlinorium (van Gool *et al.* 2002), is characterised by predominant SSE dips (in orange), while NNW dips (in blue) prevail to the north and south. NW–SE-trending foliations are predominant in two distinct areas in the north-east: one in the extreme north-eastern corner with predominating NE-dipping foliations (in red), and another around Sydostbugten, characterised by SW-dipping foliations (in green). Farther south only two areas of uniform dip directions are recognised, one around Attu with predominant SW dips (in green), and another forming a belt north of the Nordre Strømfjord shear zone, which has uniform NW dips (in blue).

Fig. 8A. Characterisation of structural domains from Fig. 2 with stereographic projections of foliations within each domain. Poles to foliations plotted on lower hemisphere, equal angle nets and contoured at 1, 2, 3, etc. times random distribution. The number of data points (**n**) and orientation of maximum density are indicated for each plot. **FA**, calculated fold axis.
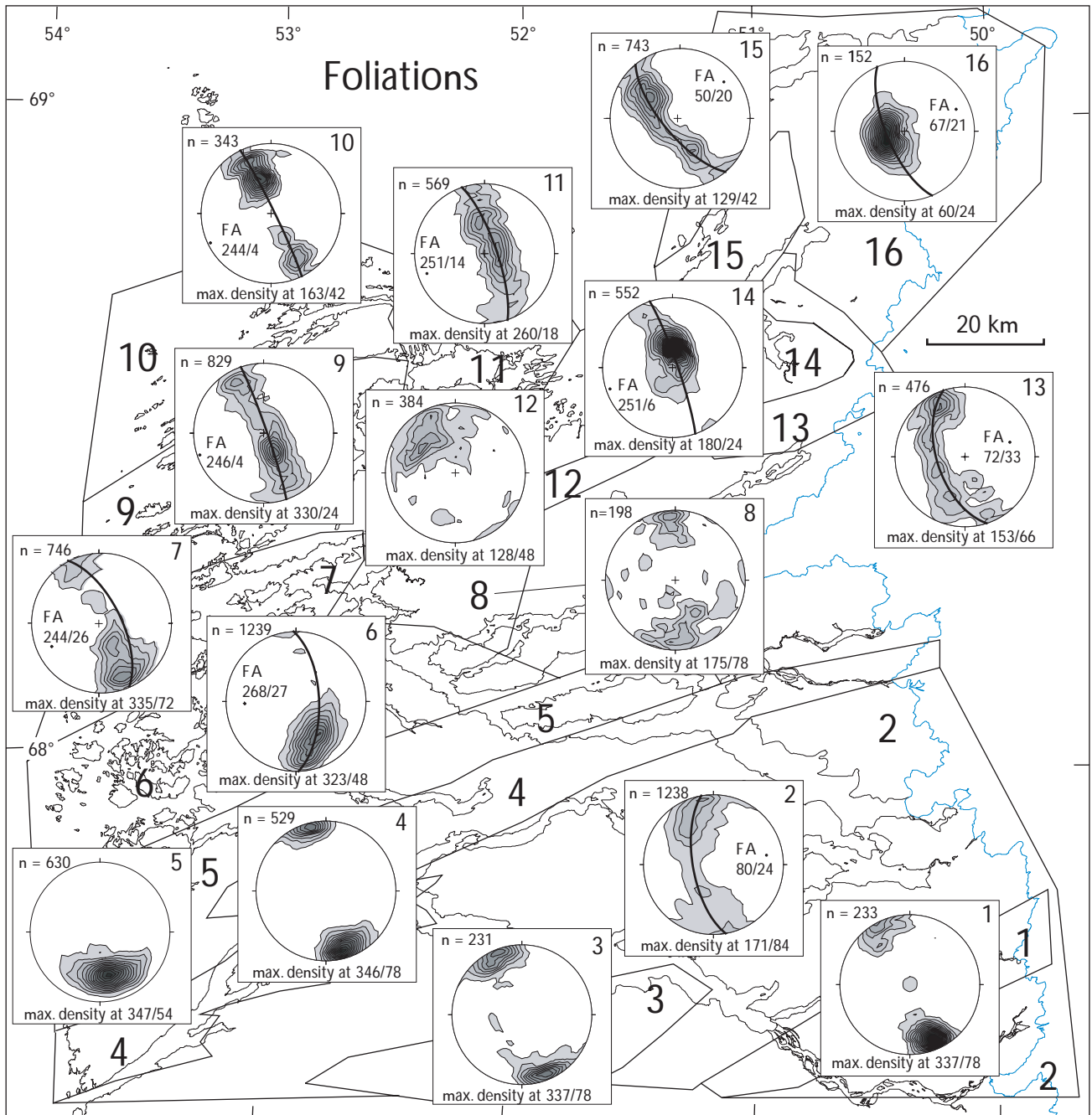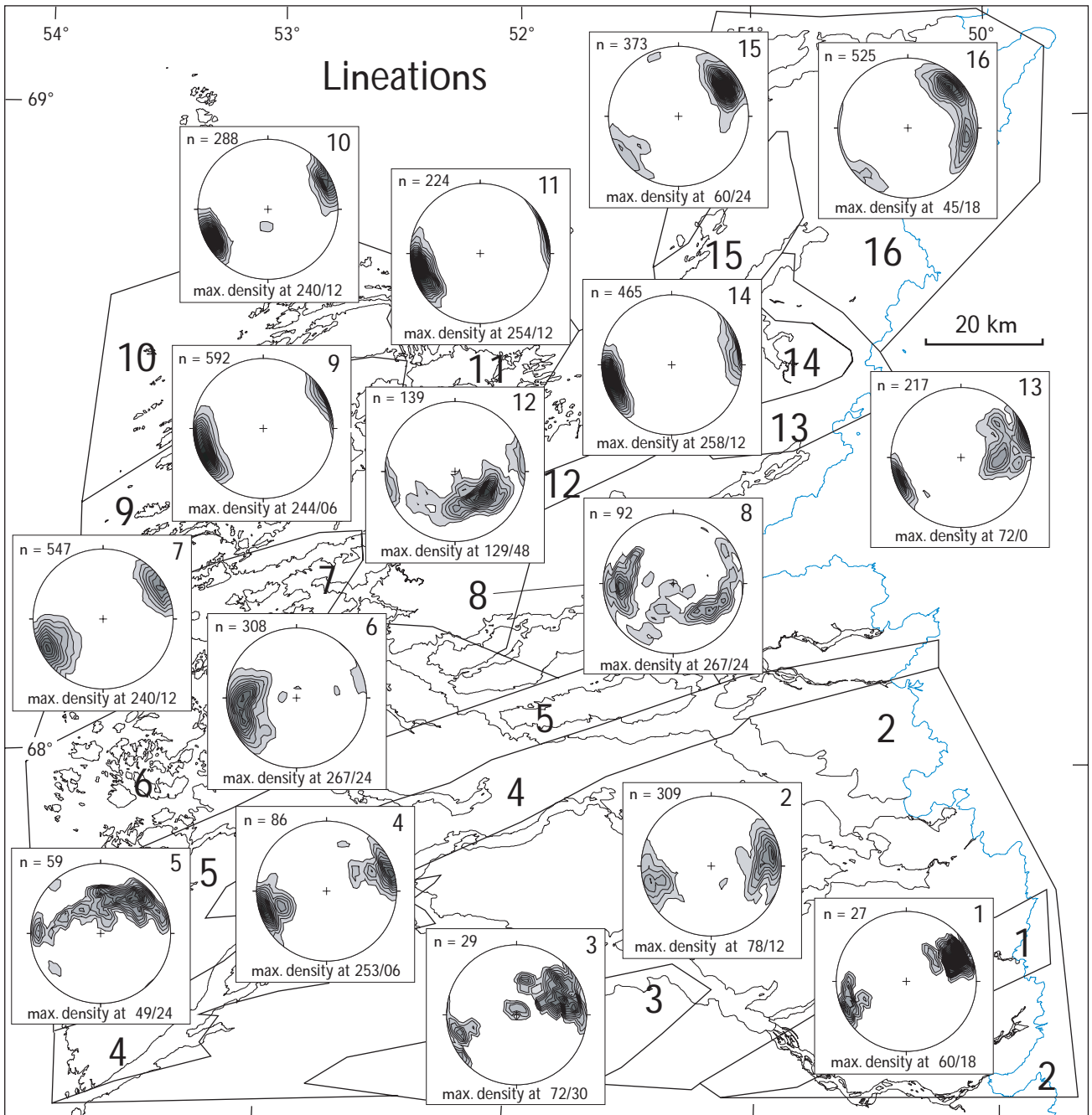
Fig. 8B. Characterisation of structural domains from Fig. 2 with stereographic projections of lineations within each domain. Data plotted on lower hemisphere, equal angle nets and contoured at 1, 2, 3, etc. times random distribution. The number of data points (**n**) and orientation of maximum density are indicated for each plot.

Table 1. Summary of characteristic features of the structural domains

Domain	Foliation	Lineation	Geology	Synopsis
1	Steep N-dipping foliation with consistent orientation. A sharp transition to S-dipping foliations at the northern boundary of the belt.	Consistent, predominant shallow ENE plunge.	Nordre Isortoq steep belt (shear zone), predominant sinistral shear. Mainly paragneiss.	High-strain strike-slip zone constrained by metasedimentary rocks.
2	Foliation curved along shallowly ENE-plunging folds on a scale of tens of kilometres. Dips variable, SE dips predominating over NE and less common SW dips.	Variable lineations, with predominant shallow ENE plunges, parallel with fold axes. Shallow, SE-plunging lineations in a c. 10 km wide zone south of the NSSZ.	Northern CNO flat belt of interleaved Archaean orthogneisses and Proterozoic ortho- and paragneisses.	Anticlinorium between two shear zones. Lineation constant in spite of intense folding. Only one zone where lineations plunge SE, locally steeply.
3	Steep foliation. Both northerly and southerly dips. Few folds on scales of 0.5–1 km.	Lineations mainly shallowly ENE-plunging. Some variation in fold hinges, especially near the eastern domain boundary.	Steep belt within the northern CNO flat belt; tightly interleaved ortho- and paragneisses.	Steep zone with tight folds within the larger domain 2 with large fold structures. Steep zone discontinuous to the east, and concentrated in an area dominated by two metasedimentary belts.
4	Steep foliations with consistent orientations, slightly oblique to the trend of the linear belt. Northerly dips predominate. Near the southern boundary a sharp transition to SSE-dipping foliations.	Subhorizontal lineations, the majority WSW-plunging in contrast with surrounding areas.	NSSZ. Interleaved ortho- and paragneisses.	Sinistral strike slip zone 5 km wide. Obliquity of foliation fits with sinistral shear.
5	Gradual northward transition from steep dips close to the NSSZ to shallower NNW dips. The foliation locally curves into the shear zone. NE dips are mixed with the dominant NNW dips in most of the area. The plentiful data points on the stereonet (Fig. 8A) obscure orientations (mainly NE-dipping) away from the maximum.	Progressive change from shallow ENE plunges near the NSSZ towards steep NE and N plunges in the north-west.	Archaean orthogneisses and horizons of supracrustal amphibolite.	Region with shallow, N-dipping structures.
6	Intensely folded region with 5–10 km large folds, mainly W-plunging. Northerly and westerly dips predominate in contrast to domain 5.	Mixed orientations with a cluster of shallowly SE-plunging lineations. In the west progressive change in orientation continues from domain 5. More variable orientations in the east.	Archaean indentor, ortho- and paragneiss as in domain 5. Large fold structures.	Overall W- and WSW-plunging folds. Two sets of lineations, one variable, the other consistently WSW-plunging, parallel with fold axis.
7	Variable strike. NNW dips less predominant than in domain 5. Folding. Dips mainly moderate, but steep in the south-west. Fig. 8A displays a girdle over shallow, WSW-plunging fold structures. A calculated great circle is discordant to the measured maxima, which align on a steeper great circle.	Rather consistent ENE-trending lineations. ENE plunges in the east become shallower and mixed with WSW-plunging domains in the west, followed by moderate to steep WSW plunges at the coast. Locally steep lineations in fold cores.	Archaean orthogneisses and metasedimentary rocks define a poorly sampled linear zone at the northern boundary of the indentor block of Piazolo et al. (2004). A few kilometre-sized fold structures.	Predominantly straight and steep foliations with ENE trends, but variable dip directions, and consistently shallow lineations. Misalignment of foliation girdle and calculated great circle (Fig. 8A) indicates complex fold pattern: along-strike variation of lineations (and presumably fold axes) and local folds with steep axes disturb the stereographic plot. Non-consistent dip directions and dips in the northern linear zone suggest intense folding.
8	Foliations outline the large fold structure visible on Fig. 1. Southerly dips predominate in the northern part (green and orange/brown, Fig. 3A). A zone with NW dips (blue) runs through the domain centre. Mixed dip directions in the south. Dips moderate to steep. Irregular stereonet pattern (Fig. 8A), with remnants of a great circle distribution similar to that in domains 6 and 7.	Steep SW- and SE-plunging lineations around a large central fold core. Mainly E–W-trending lineations in the west in transition to domain 7. Variable lineations in the east. Two maxima of shallow W plunges and steeper SE plunges (Fig. 8B), the latter possibly with a small circle distribution.	Orthogneisses interleaved with supracrustal amphibolite. A fold interference pattern occurs south of the main fold at the western end of the Naternaq belt.	Mixed structural patterns including ENE-trending fold limbs and fold interference patterns. The core of the large fold with the steep lineations is located along the southern extension of a NNE-trending belt of steep lineations on the western limb of the Naternaq supracrustal belt.

CNO: Central Nagssugtoqidian orogen. NNO: Northern Nagssugtoqidian orogen. NSSZ: Nordre Strømfjord shear zone.

Table 1 (*continued*)

Domain	Foliation	Lineation	Geology	Synopsis
9	Consistent ENE trend with both NNW and SSE dip directions. Large fold structures in the east. Steep dips, shallower towards north. Great circle distribution with shallowly NNW-dipping and subordinate steep, SSW-dipping flanks tentatively interpreted as due to asymmetric S-vergent folds (Fig. 8A).	Predominant subhorizontal ENE–WSW-trending lineations, gradually changing to E–W in the east, where large-scale folds occur. Very strong preferred ENE–WSW subhorizontal orientation, with a tail towards E–W trends displayed on Fig. 8B.	Region around Kangaatsiaq with metasedimentary rocks, amphibolite and granite within the regional grey gneiss.	Transition from predominant steep, northerly dips in the CNO to shallower, variable dips and large fold structures in the north. From east to west a large swing from ENE–SSW to E–W trends. Lineations uniform also in the area of large folds.
10	Mainly steep S dips with consistent trend. As in domain 9, ENE-WSW-trending foliation in the west swings towards E–W in the east. At the southern boundary a linear belt with moderate S dip. Partial great circle distribution; no dip directions within the NE quadrant (Fig. 8A).	Consistent ENE–WSW-trending subhorizontal lineations, with indistinct domains of respectively easterly and westerly plunges. Strong point maximum on stereonet with shallow WSW plunges (Fig. 8B).	Straight zone of pre-dominant orthogneisses around Aasiaat, bounded to the south by a high-strain zone.	Very consistent foliation trends, the northernmost widespread steeply dipping foliations, and very persistent lineations.
11	Foliations outline a W-plunging antiform *c.* 10 km large. The northern part of its northern limb appears overturned towards N. Great circle distribution with predominant shallow to moderate dips on stereonet (Fig. 8A).	Shallow plunges of lineations, mainly towards W. Subordinate NW plunges on northern fold limb. Fig. 8B shows strong point maximum parallel with calculated fold axis.	Ikamiut supracrustal rocks. Large antiform with 1 km-scale parasitic folds on its southern limb. Northern limb poorly exposed and undersampled.	Data consistent with a shallowly W-plunging antiform becoming progressively tighter westward (but not easily traced into domain 10).
12	Foliations outline a fold with a folded, overall moderately SE-dipping western main limb. The high-strain southern limb dips steeply S. Large spread on stereonet (Fig. 8A).	Moderately SE-plunging lineations on the western limb, with isolated SSW plunges in hinge zone. Very few measurements on the southern limb, with shallow WSW plunges.	Western Naternaq belt. Steep paragneisses folded on 20 km-scale. Mainly data from isoclinal fold on western limb; less from straight southern limb.	Western limb of Naternaq supracrustal belt, forming a distinct zone, apparently transecting the overall ENE-trending fabric, and with uncommon SE-plunging lineations and fold axes.
13	Eastern continuation of steep, high-strain southern limb of fold from domain 12 and large E-plunging antiform. NW dips more common in the north, dips shallower near hinge. The northern limb has moderate to steep NE dip. Fig. 8A shows a well-defined great circle and NE-plunging calculated fold axis.	Lineations shallow and ENE- or WSW-plunging on the southern limb. Variable plunges on the eastern limb between NE and ESE. The latter orientation most common in hinge areas. Fig. 8B clearly shows these three separate populations.	Steeply dipping, straight gneisses in eastern Naternaq belt. A large E-plunging antiform at the eastern end, and a north-eastern fold limb with only minor meta-sedimentary rocks.	Consistent lineation trend in antiform, but opposite plunge directions on the limbs. Steeper lineations in the fold hinge.
14	Irregular foliation in the core of the eastern Naternaq fold, forming an E–W-trending whaleback structure. Fig. 8A shows a point maximum and partial girdle which do not fit the calculated great circle (see the main text).	Predominant subhorizontal WSW plunges, except ENE plunges at the eastern domain margin along the eastern limb of the map-scale fold. Fig. 8B shows a single strong point maximum.	Predominantly ortho-gneiss, cut by flat-lying shear zones.	Very consistent lineation trends, also through the antiform in the east. Direction of plunge flips over in the east, perhaps indicating two generations of lineations.
15	Foliations define a large, open NE-trending synform with steepest orientations in the core, bounded by straight belts. An antiform occurs in the south-east, with its southern limb in domain 13. A well-defined great circle on Fig. 8A indicates cylindrical, NE-plunging folds.	Strong predominance of ENE-plunging lineations along the synform axis. Consistent SE plunges south-east of the shear zone. Consistent moderate NW plunge in the antiform near head of fjord. Fig. 8B shows a fairly well defined point maximum close to the calculated fold axis.	Synform with strongly migmatitic paragneiss and a core of migmatitic orthogneiss. High-strain zones to the north-west and south-east.	The south-eastern limb of the synform, overturned to the north-west and becoming very tight towards north-east. Distinctly different lineations in the underlying, folded shear zone.
16	The foliation defines large, open, NE-plunging folds besides a large antiform surrounding the synform of domain 15. The stereonet data (Fig. 8A) display a point maximum with a partial great circle distribution.	Predominant shallow, NE-plunging lineations and a small population of slightly steeper, E-plunging lineations in the north-eastern domain corner. The lineations swing, following the folds.	Archaean orthogneiss with thin sheets of pelitic rocks and supracrustal amphibolite. Also areas of very weakly foliated porphyritic granodiorite.	The NE-dipping orientations and open folds are significantly different from elsewhere in NNO. The shear zone exposed on either side of the synform in domain 15 does not continue in domain 16.

The stereographic projections of the foliations clearly reflect two trends (Fig. 8A). The plots from the southern part of the study area define alternating point maxima and great circle distributions, reflecting, respectively, the linear belts and the fold-dominated regions. In contrast, in most of the NNO the plots mainly display (partial) great circle distributions or otherwise irregular patterns, indicating the lack of extensive linear belts in the north. Furthermore, the stereographic projections reflect the northward decrease in dip angle: in the CNO the point maxima indicate dip angles around 80°, whereas the NNO is characterised by point maxima indicating dip angles in the range 20–40°.

Lineations

Overviews of the linear fabrics are shown in Figs 5, 6. The highly uneven data density in the lineation maps (Fig. 5A, B) reflects that the southern and northern parts of these maps have been compiled from different sources, i.e. published maps in the south and complete field datasets in the north. Nevertheless, it is apparent that the dominant trend is ENE–WSW, as indicated by the predominant red and green colours (Fig. 5). Outside the linear belts, gradual changes in the lineation trends on a scale of 10–50 km or more are seen, for example between Attu and Nordre Strømfjord, at western Ussuit, and in the north-east of the study area. Several smaller areas are dominated by E–W trends, for example east of Attu, south-east of Sydostbugten, and south of Jakobshavn Isfjord.

Most lineations plunge 0–30°, with markedly steeper plunges in regions of map-scale fold interference structures and fold hinges. This is prominent west of Ataneq, north-west of Attu, and in the eastern part of domain 13. These regions are also characterised by orientations that diverge from the general ENE–WSW trend.

The structural maps (Fig. 6) stereographic projections (Fig. 8B) clearly show that WSW-plunging lineations predominate in most of the NNO (north of the Nordre Strømfjord shear zone) except for small clusters of NE-plunging lineations and the area east and north-east of Sydostbugten, where the plunge is towards ENE (domains 13, 15 and 16); there is a sharp break between these two plunge directions east of Sydostbugten. The same pattern is shown by the fold axes calculated from the great circle girdles of the foliations (Fig. 8A). South of the Nordre Strømfjord shear zone (in the CNO), the point maxima of the lineations and calculated fold axes consistently indicate shallow ENE plunges.

Fold axes

Orientations of fold axes are shown on Fig. 7. The symbols are colour-coded for plunge angle in order to facilitate comparison with the lineation data. The orientations of the fold axes mimic the general characteristics of the lineations, being generally subparallel with the latter. Their distribution in clusters reflects a higher density of measurements in areas of map-scale fold hinges, where outcrop-scale folds are more common.

Tectonic implications

The structural data presented in this paper show that the tectonic style changes significantly across the central and northern parts of the Nagssugtoqidian orogen. While the CNO is dominated by steep, linear and continuous belts separated by well-defined areas of large-scale folding, the NNO does not contain such continuous, linear belts, whereas 20–80 km-scale folds are abundant. The main change in tectonic style occurs across the Nordre Strømfjord shear zone. More specifically, the southern part of the study area (the CNO and the Nordre Strømfjord shear zone) is dominated by alternating linear belts and folded regions. The corresponding structural domains follow the main strike of the linear belts and are continuous from the coast to the Inland Ice. The linear belts themselves are dominated by sinistral strike-slip deformation. In contrast, the domains in the NNO are generally less elongate and reflect the lack of linear belts of similar dimensions as in the CNO. Small high-strain zones are observed locally, e.g. along the northern and southern margins of domain 15 and with several examples in domains 7, 9 and 10. Shear sense indicators are rare and inconsistent in the NNO, and the overall deformation in this region seems to be predominantly coaxial (Piazolo *et al.* 2004; Mazur *et al.* 2006, this volume). The change in tectonic style is interpreted to be a result of (a) differences in localisation of strain as high-strain, steep belts, (b) different deformation kinematics (strike-slip wrench tectonics in the south, coaxial deformation in the north), and (c) variations in the intensity of deformation. We consider that the overall Palaeoproterozoic strain is significantly lower in the NNO than in the CNO. The NNO commonly preserves shallow dips, which presumably predominated after the original phase of thrusting. Besides, the two latest deformation phases, which are responsible for the steep foliation in the CNO, are less intense in the NNO (van Gool *et al.* 2002; Piazolo *et al.* 2004; Mazur *et al.* 2006, this volume). These observations may account for the previously

outlined differences in the mode of strain localisation. The data presented here furthermore show that the change in style is rather abrupt across the Nordre Strømfjord shear zone, and thus support the interpretation by Sørensen (1983) and Sørensen *et al.* (2006, this volume) that this structure is of crustal scale and has a significant offset – a notion that has previously been questioned by Hanmer *et al.* (1997).

It is well established in the literature that the structural pattern of the CNO is fully attributed to Nagssugtoqidian deformation (van Gool *et al.* 2002). In contrast, the NNO is currently interpreted as having only in part been affected by Palaeoproterozoic deformation, and the Nagssugtoqidian strain is furthermore partitioned into smaller regions (Piazolo *et al.* 2004; Mazur *et al.* 2006, this volume). A significant part of the deformation in the NNO thus seems to be of Archaean age, and its overall structural style defined by interference between Archaean and Palaeoproterozoic structures. Therefore, like Mazur *et al.* (2006, this volume) we suggest that the change in tectonic style from south to north reflects partitioning of Nagssugtoqidian strain. This is clearly illustrated by the smaller and less elongate structural domains in the NNO, and by the significant change of the general trend of both foliations and lineations towards the north-eastern corner of the study area, where we consider that the influence of the Palaeoproterozoic deformation diminishes rapidly. This interpretation is supported by the relatively low metamorphic temperatures recorded by Hollis *et al.* (2006, this volume) in some parts of the NNO.

It is beyond the scope of this contribution to explore the details of the structural domains that we have outlined. However, three other contributions in the present volume of Geological Survey of Denmark and Greenland Bulletin deal with the specific nature of some of these domains. Sørensen *et al.* (2006, this volume) investigate the character of the Nordre Strømfjord shear zone and adjacent areas in domains 4 and 5, Mazur *et al.* (2006, this volume) focus on the partioning of structures within domains 6, 7 and 8, and Hollis *et al.* (2006, this volume) describe structures within domains 11 and 15.

Conclusions

The application of a GIS computer program enables us to visualise large amounts of structural data in a variety of ways. Thus, we can rapidly obtain an overview of large datasets that are otherwise difficult to manage, and delineate areas with consistent tectonic trends. Although the methods applied here de not reveal features that are not present in the original geological maps, they can substantially facilitate the detection and description of structural trends and variations. In addition, stereographic plots of each of the domains can quickly be produced and analysed. In the present case, the methods greatly helped to subdivide the central and northern Nagssugtoqidian orogen into distinct structural domains with specific individual characters.

The investigation of the large-scale structural trends in the central and northern Nagssugtoqidian orogen revealed distinct changes in the tectonic style from south to north. In the core of the orogen, the ENE-striking Nordre Strømfjord shear zone from the coast to the Inland Ice forms the most prominent feature. The tectonic character of the orogen changes across this structure from predominantly ENE-tending, steep fabrics in the south to large fold patterns and generally flat structures in the north, with a marked decrease in the main dip angle from *c.* 80° south of the shear zone, to *c.* 20–40° in the north. In addition, a significant decrease in the intensity of deformation is apparent, coupled with a decreasing proportion of the strain localised in linear belts. We interpret these patterns as reflecting a general northward decrease in the Palaeoproterozoic tectonic overprint on Archaean structures, as well as strain partitioning in smaller regions. Hence, some of the structural domains in the NNO are largely unaffected by pervasive Palaeoproterozoic deformation.

References

Bonham-Carter, G.F., Agterberg, F.P. & Wright. D.F. 1990: Weights of evidence modelling: a new approach to mapping mineral potential. Geological Survey of Canada Paper **89**, 171–183.

Books, C.J. 2000: Defining groundwater system recharge and vulnerability areas in regions of suburban expansion; overview of the northern Illinois example. Abstracts with Programs – Geological Society of America **33**, 45 only.

Carrasco, M.A. & Barnosky, A.D. 2000: MIOMAP: a GIS-linked database to assess the effects of tectonic and climatic changes on mammalian evolution. Abstracts with Programs – Geological Society of America **32**, 15 only.

Connelly, J.N., van Gool, J.A.M. & Mengel F.C. 2000. Temporal evolution of a deeply eroded orogen: the Nagssugtoqidian orogen, West Greenland. Canadian Journal of Earth Sciences **37**, 1121–1142.

Goodwin, P.B, Choiniere, M.E., Harris, F.W. & Dean, B.P. 1996: Im-

proving exploration with geographical information system (GIS) technology. American Association of Petroleum Geologists Bulletin **80**, 1297.

Hanmer, S., Mengel, F., Connelly, J. & van Gool, J.[A.M.] 1997: Significance of crustal-scale shear zones and syn-kinematic mafic dykes in the Nagssugtoqidian orogen, SW Greenland: a re-examination. Journal of Structural Geology **19**, 59–75.

Harris, J.R., Wilkinson, K., Heather, K., Fumerton, S., Bernier, M.A., Ayer, J. & Dahn, R. 2001: Application of GIS processing techniques for producing mineral prospectivity maps – A case study: mesothermal Au in the Swayze Greenstone Belt, Ontario, Canada. Natural Resources Research **10**, 91–124.

Hollis, J.A., Keiding, M., Stensgaard, B.M., van Gool, J.A.M. & Garde, A.A. 2006: Evolution of Neoarchaean supracrustal belts at the northern margin of the North Atlantic Craton, West Greenland. In: Garde, A.A. & Kalsbeek, F. (eds): Precambrian crustal evolution and Cretaceous–Palaeogene faulting in West Greenland. Geological Survey of Denmark and Greenland Bulletin **11**, 9–31 (this volume).

Kalsbeek, F. & Nutman, A.P. 1996: Anatomy of the Early Proterozoic Nagssugtoqidian orogen, West Greenland, explored by reconnaissance SHRIMP U-Pb dating. Geology **24**, 515–518.

Knox-Robinson, C.M. & Weyborn, L.A.I. 1997: Towards a holistic exploration strategy: using geographic information systems (GIS) as a tool to enhance exploration. Australian Journal of Earth Sciences **44**, 453–463.

Manatschal, G., Ulfbeck, D. & van Gool, J.[A.M.] 1998. Change from thrusting to syncollisional extension at a mid-crustal level: an example from the Palaeoproterozoic Nagssugtoqidian orogen (West Greenland). Canadian Journal of Earth Sciences **35**, 802–819.

Marker, M., Mengel, F., van Gool, J. & field party 1995: Evolution of the Palaeoproterozoic Nagssugtoqidian orogen: DLC investigations in West Greenland. Rapport Grønlands Geologiske Undersøgelse **165**, 100–105.

Mazur, S., Piazolo, S. & Alsop, G.I. 2006: Structural analysis of the northern Nagssugtoqidian orogen, West Greenland: an example of complex tectonic patterns in reworked high-grade metamorphic terrains. In: Garde, A.A. & Kalsbeek, F. (eds): Precambrian crustal evolution and Cretaceous–Palaeogene faulting in West Greenland. Geo-

logical Survey of Denmark and Greenland Bulletin **11**, 163–178 (this volume).

Olesen, N.Ø. 1984: Geological map of Greenland, 1:100 000, Agto 67 V.1 Nord. Copenhagen: Geological Survey of Greenland.

Piazolo, S., Alsop, G.I., van Gool, J.A.M. & Nielsen, B.M. 2004: Using GIS to unravel high strain patterns in high grade terranes: a case study of indentor tectonics from West Greenland In: Alsop, G.I. *et al.* (eds.): Flow processes in faults and shear zones. Geological Society Special Publication (London) **224**, 63–78.

Sørensen, K. 1983: Growth and dynamics of the Nordre Strømfjord Shear Zone. Journal of Geophysical Research **88**, 3419–3437.

Sørensen, K., Glassley, W., Korstgård, J. & Stensgaard, B.M. 2006: The Nordre Strømfjord shear zone and the Arfersiorfik quartz diorite in Arfersiorfik, the Nagssugtoqidian orogen, West Greenland. In: Garde, A.A. & Kalsbeek, F. (eds): Precambrian crustal evolution and Cretaceous–Palaeogene faulting in West Greenland. Geological Survey of Denmark and Greenland Bulletin **11**, 145–161 (this volume).

True, M.A., Slawski, J.J. & Hibner, B.A. 1999: Assessment of environmental hazards in western Siberian oil fields using remotely sensed imagery from U.S. and Russian national security systems. Proceedings of the Thematic Conference on Geologic Remote Sensing **13**, 13–20.

van Gool, J.A.M. & Marker, M. 2004: Geological map of Greenland, 1:100 000, Ussuit 67 V.2 Nord. Copenhagen: Geological Survey of Denmark and Greenland.

van Gool, J.A.M., Connelly, J.N., Marker, M. & Mengel, F.C. 2002: The Nagssugtoqidian orogen of West Greenland: tectonic evolution and regional correlations from a West Greenland perspective. Canadian Journal of Earth Sciences **39**, 665–686.

Vollmer, F.W. 1990: An application of eigenvalue methods to structural domain analysis. Geological Society of America Bulletin **102**, 786–791.

Wilson, C.E., Scott, H.D., Norman, R.J., Slaton, N.A. & Frizzell, D.L. 2000: Spatial distribution of irrigation water quality parameters in Desha County, Arkansas. Abstracts with Programs, Geological Society of America **32**, 45 only.